Eur. Phys. J. Appl. Phys. **97**, 53 (2022)

https://doi.org/10.1051/epjap/2022220076

THE EUROPEAN PHYSICAL JOURNAL APPLIED PHYSICS

Regular Article

Effective optical path length measurement of integrating cavity using time-resolved spectroscopy and tunable diode laser absorption spectroscopy

Xue Zhou*, Haiwei Li, and Peng Hu

School of Computer Science and Information Engineering, Chongqing Technology and Business University, Chongqing 400067, P.R. China

Received: 20 March 2022 / Received in final form: 31 May 2022 / Accepted: 18 July 2022

Abstract. Integrating cavities are commonly used in trace gas detection and weak absorption measurement. The effective path length (L) is an important index for evaluating the ability to increase the optical path length of an integrating cavity. Studies have demonstrated that the effective path length (L) is related to the inner surface reflectivity, cavity shape and dimension, and port fraction. However, the measured effective path length (L) of an integrating cavity generally varies with the spectroscopic technique used in practical applications. In this study, the effective path lengths (L) of a cubic integrating cavity with different port fractions were measured using time-resolved spectroscopy and tunable diode laser absorption spectroscopy (TDLAS). The value of L gradually decreased with an increase in the port fraction. Further, the measured L results showed a deviation between the two measurement techniques. The reason for the different effective optical paths obtained by the two spectroscopic techniques was investigated. An analysis showed that the difference in the effective optical paths was due to the reflectivity difference at the different laser wavelengths used for the two spectral methods. Correcting the reflectivity eliminates the difference in the effective optical paths.

1 Introduction

Integrating cavities are often used in trace gas detection and weak absorption measurement to extend the optical path length and thereby increase the absorption signal of a sample [1,2]. If the inner wall is covered with a coating with high diffuse reflectivity, forming an ideal Lambertian surface, after multiple scattering, the input light can form an isotropic light field and achieve a long optical path. Integrating cavities feature a simple structure and good stability, with no need to precisely align the laser beam [3]. In addition, their most attractive characteristic is their low cost, which gives diffuse cavities very good potential for commercial production and application as gas cells with improved detection sensitivity [4,5]. Because of these special advantages, integrating cavities have been employed in many spectroscopic techniques, such as tunable diode laser absorption spectroscopy (TDLAS) and cavity-enhanced spectroscopy [6–8]. In particular, Bixler et al. present a technique for detecting trace amounts of human or animal waste products in water using cavity-enhanced spectroscopy, which could allow for the real-time assessment of water quality without the need for expensive laboratory equipment by employing an integrating cavity [8].

The effective path length (L) is an important parameter for evaluating an integrating cavity's ability to increase the optical path length. Many researchers have studied the effective path length (L) of an integrating cavity [9–11], which can be expressed as follows:

$$L = L_0 + \frac{\rho}{1-\rho(1-f)}\,\overline{d}\,. \tag{1}$$

Here, ρ is the diffuse reflectivity of the inner wall coating; f is the port fraction (the ratio of all the port areas to the inner surface area); $\overline{d}$ is the single-pass average path length between successive reflections, and it has been found that $\overline{d} = 4V/S$, where V is the volume of the cavity and S is the inner surface area; and L_0 is an extra path length produced by the emission conditions, which has been verified as the diameter for an integrating sphere and the side length of a cubic integrating cavity [12].

Equation (1) is generally true in both broadband measurement and TDLAS, where continuous wave illumination is often applied as the light source. However, when a pulse laser is used as the light source, such as for cavity-enhanced spectroscopy and integrating cavity ring down spectroscopy (ICRDS) [13,7]. A study should be conducted to determine whether effective path length L can still be found using equation (1) for a pulse source.

In this study, a 35 cm cubic diffused integrating cavity was developed. It had a removable top lid to obtain different port fractions. The effective path lengths (L) of the cubic integrating cavity with different port fractions were measured based on time-resolved spectroscopy and TDLAS. The two sets of effective path length (L) values

* e-mail: zhouxue@ctbu.edu.cn

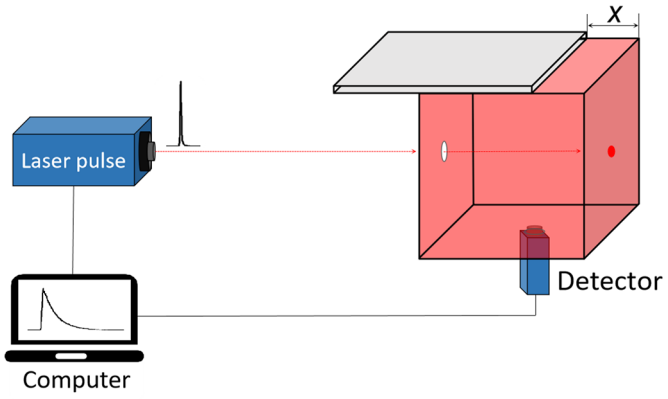

Fig. 1. Experimental setup of time-resolved spectroscopy.

were analysed, and the difference was corrected by considering the laser wavelength.

2 Experiments and results

2.1 Time-resolved spectroscopy

The experimental setup for the time-resolved spectroscopy is shown in Figure 1. The cubic integrating cavity was made with 3 mm thick stainless steel plates. The diameter of the in/output diaphragm was 2 mm. The inner walls of the cavity were coated with 0.4 mm thick Avian-D paint (Avian Technologies LLC). The reflectivity of this coating is 98.3–98.5% at a wavelength of 700–800 nm, based on the manufacturer's technical brochures [14]. A laser (NKTPhotonics-Superk Extreme) that emitted a pulse with an output power of 300 mW and output frequency of 2 MHz was used as the light source. The output light was detected by a photon counter (Becker & Hickl GmbH, PMC-100-1). To prevent absorption of the gases in the air, a laser wavelength of 710 nm was selected.

Moving the top lid by distance x from the side wall added port fraction f_x to the original port fraction f_0. The sum of the original and added port fractions became the total port fraction: $f = f_0 + f_x$. Figure 2 shows the input and output pulse curves for different port fractions. The pulse width of the input laser was approximately 0.7 ns. The curves were normalised to make the pulse curves comparable.

Based on time-resolved spectroscopy, the incident light pulse first led to a homogeneous field via repeated diffusion by the inner surface. Then, the light intensity decayed as a function in exponential form [15]. Decay constant τ can be obtained by function fitting, as shown in Figure 3, and L can be expressed as follows:

$$L = \tau \cdot c, \tag{2}$$

where c is the speed of light. Thus, the L values for different port fractions could be calculated using the decay constant τ. Once the isotropic field was created, the falling edge of the output curve decayed exponentially. The rising edge of the curve was considered to be the establishment process for the isotropic field. The falling edges of the decay curves were fitted using the exponential function. Figure 3 shows the fitting process for the output decay pulse when $f_x = 0$.

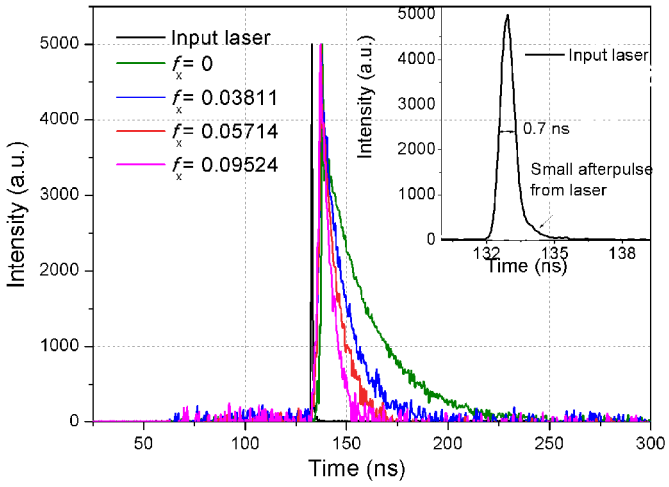

Fig. 2. Input and output pulse curves of cubic integrating cavity with different added port fractions (inset shows enlarged view of input pulse).

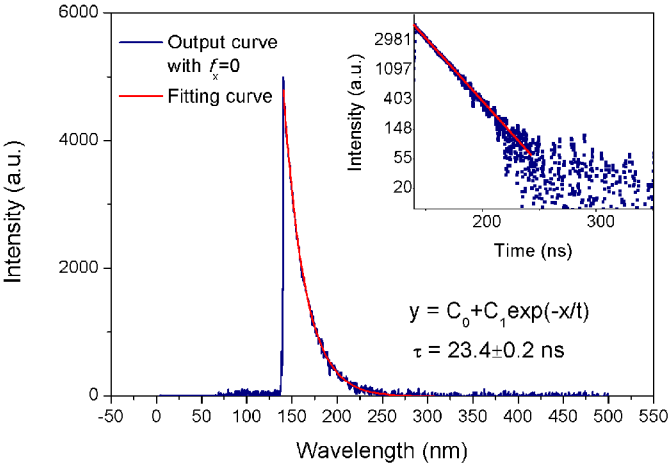

Fig. 3. Exponential fitting of output decay pulse when $f_x = 0$.

The output decay pulses for different added port fractions are exponentially fit. Based on the fitting results, the values of decay constant τ for different added port fractions could be obtained, and the corresponding L values could be calculated.

2.2 TDLAS

TDLAS is a universal gas detection technique [16–18]. An integrating cavity is commonly used as the gas absorption cell in TDLAS. The concentration of oxygen in the ambient air is stable. Thus, the effective path length (L) of a diffused integrating cavity can be calibrated by comparing the oxygen absorption signals in open air and in the integrating cavity using TDLAS. A schematic of the experiment is shown in Figure 4. The second harmonics of the oxygen absorption signals were measured by combining wavelength modulation spectroscopy with TDLAS. A vertical-cavity surface-emitting tunable diode laser (LaserComponents. Single Mode VCSEL 763 nm TO46) with a free running output power of 0.3 mW was used as the light

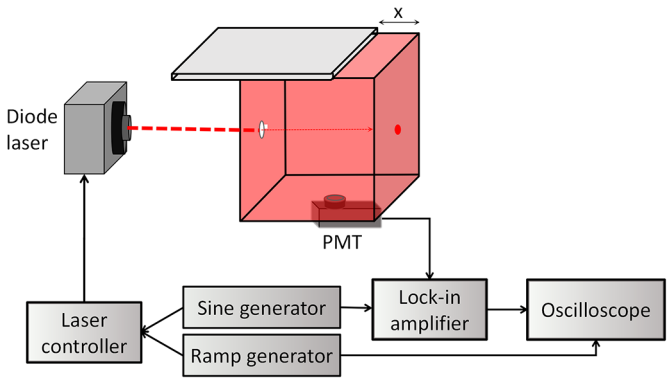

Fig. 4. Experimental setup for measuring oxygen absorption in integrating cavity using TDLAS.

source. The temperature of the laser was controlled at 22.47 °C (Thorlabs TED 200C, Temperature Controller). The laser injection current was 1.26 mA (Thorlabs LDC 200, VCSEL Laser Diode Controller), which was modulated by a superimposed signal with a sinusoidal component (4 kHz, 40 mV) and ramped component (10 Hz, 380 mV), corresponding to the current varying from 1.12 mA to 1.40 mA. The centre frequency of the laser scanned the oxygen absorption P9 line in the A-band at 763.84 nm. The output light from the integrating cavity was received by a photomultiplier tube (PMT, Hamamatsu, PMTH-S1-1P28). The signal was demodulated using a lock-in amplifier (SR830) with a 1 ms time constant at the second harmonic of the modulation frequency (2f, 8 kHz). Data were recorded and displayed by an oscilloscope (Tektronix, DPO5054). During the experiment, the temperature was controlled at 25 °C in the laboratory.

Figure 5 shows the optical parameter (OP) of the absorption signal in air and in the cavity when $f_x = 0$. The calibration curve between the OP and optical path length in the air was obtained by measuring oxygen absorption signals when the optical path length varied from 10 to 500 cm. The OP was calculated as the sum of the absolute value of the second harmonic signal. The effective path length (L) of the integrating cavity when added port fraction $f_x = 0$ was 628 cm, as shown in Figure 5. By moving the top lid of the cavity, the values of L for different added port fractions could be measured.

3 Discussion

The effective path length (L) values for the integrating cavity with different added port fractions were measured using time-resolved spectroscopy and TDLAS. Figure 6a shows the measured results and corresponding curve fit using equation (1).

The blue and red points show the experimental data measured by time-resolved spectroscopy and TDLAS, respectively. The blue and red lines are the corresponding curves of the experimental data fit using equation (1). The best fitting parameters are also shown in Figure 6a. The original port fraction was fit as 0.007. The curves fitted using

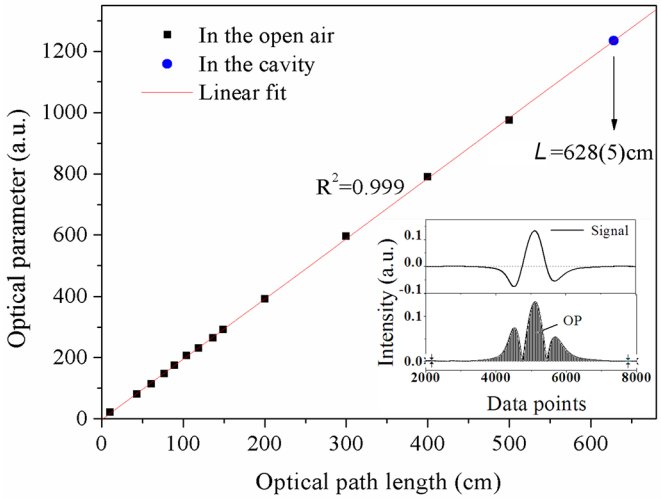

Fig. 5. Calibration curve between optical parameter (OP) and optical path length in air and integrating cavity. The inset shows an oxygen absorption second harmonic signal and the OP calibration method.

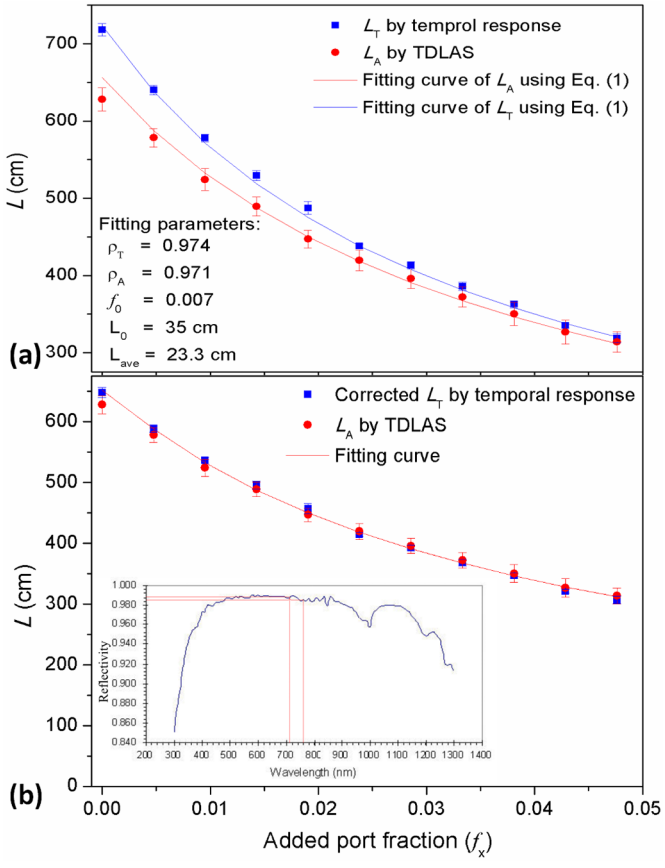

Fig. 6. (a) Experimental data and curve fit using equation (1) for different added port fractions found with time-resolved spectroscopy and TDLAS; (b) L results of two spectroscopic techniques after correction. The inset shows the reflectivity of the inner coating material (Avian-D) at different wavelengths [18].

equation (1) were in relatively good agreement with the experimental data points. With an increase in the added port fraction, the effective path length L gradually decreased.

As seen by the fitting parameters in Figure 6a, the fitted reflectivity values of the two spectral method results were different. An analysis showed that this difference in reflectivity was caused by the inner coating, which had different reflectivity values at different wavelengths. In the experiments, the laser wavelength was 710 nm for time-resolved spectroscopy and 763 nm for TDLAS. According to the reflectivity data from Avian Technologies LLC [18], as shown in the inset of Figure 6b, the reflectivity values for material Avian-D at 710 nm and 763 nm differ and can reach 98.5% and 98.3%, respectively, under ideal conditions. However, based on the experimental fitting results shown in Figure 6a, the actual reflectivity values were lower than the ideal values at 97.4% and 97.1%, respectively, which could have been caused by the application, thickness, or contamination of the paint, as well as other conditions.

A correction was introduced based on equation (1) to eliminate the deviation between the two spectral methods, as shown in Figure 6b. After correction, the L values measured by the two spectral methods agreed well and both followed equation (1). This demonstrates that the effective path length (L) of an integrating cavity is fixed and invariant when using different spectral techniques. Moreover, equation (1) for effective path length L is universally valid for different spectroscopic applications.

4 Conclusion

A cubic diffused integrating cavity was developed, where the top lid was designed to be removable to change the port fraction added to the cavity. The effective path length (L) values of the cavity with different port fractions were measured using time-resolved spectroscopy and TDLAS. A difference was found between the measured L results of the two spectral methods. Equation fitting was implemented for the measured L results based on equation (1). The fitting reflectivity values were different for the two spectral results because the inner coating had different reflectivity values at different laser wavelengths. After reflectivity correction, the L results of the two spectral methods were in agreement. Thus, the effective path length (L) of an integrating cavity is fixed and invariant for different spectral techniques. Moreover, equation (1) for effective path length L is universally valid for different spectroscopic applications.

This work was supported by the Chongqing Natural Science Foundation (grant No. cstc2021jcyj-msxmX0627), the Science and Technology Research Program of the Chongqing Municipal Education Commission (grant No. KJQN202000829), Research Fund of High-Level Talent from Chongqing Technology and Business University (No. 1956045), and Chongqing Technology and Business University Project (No. 2152029).

Author contribution statement

Xue Zhou conceived the idea and proposed the methodology. Xue Zhou, Haiwei Li and Peng Hu implemented the experimental investigations, performed the data analysis and wrote the manuscript. Xue Zhou supervised the work. All the authors contributed to the discussion and to finalizing the manuscript.

References

1. J.N. Bixler, C.A. Winkler, B.H. Hokr, J.D. Mason, V.V. Yakovlev, J. Mode. Opt. **63**, 76 (2016)
2. E.S. Fry, J.D. Mason, Phys. Scr. **91**, 043004 (2016)
3. J. Hodgkinson, D. Masiyano, R.P. Tatam, Appl. Phys. B **110**, 223 (2013)
4. J. Yu, F. Zheng, Q. Gao, Y.J. Li, Y.G. Zhang, Z.G. Zhang, S. H. Wu, Appl. Phys. B **110**, 223 (2013)
5. E. Hawe, C. Fitzpatrick, P. Chambers, G. Dooly, E. Lewis, Sens. Actuators, A **141**, 414 (2008)
6. E. Hawe, C. Fitzpatrick, P. Chambers, E. Lewis, J. Opt. A: Pure Appl. Opt. **9**, S12 (2007)
7. M.T. Cone, J.D. Mason, E. Figueroa, B.H. Hokr, J.N. Bixler, C.C. Castellanos, G.D. Noojin, J.C. Wigle, B.A. Rockwell, V.V. Akovlev, E.S. Fry, Optica **2**, 162 (2015)
8. J.N. Bixler, M.T. Cone, B.H. Hokr, J.D. Mason, E. Figueroa, E.S. Fry, V.V. Yakovlev, M.O. Scully, PNAS **111**, 7208 (2014)
9. S. Bergin, J. Hodgkinson, D. Francis, R.P. Tatam, Opt. Express **24**, 13647 (2016)
10. Labsphere Inc. A guide to integrating sphere theory and applications (1994), http://www.labsphere.com
11. J. Yu, Y.G. Zhang, Q. Gao, G. Hu, Z.G. Zhang, S.H. Wu, Opt. Lett. **39**, 1941 (2014)
12. J. Hodgkinson, D. Masiyano, R.P. Tatam, Appl. Opt. **48**, 5748 (2009)
13. M.T. Cone, J.A. Musser, E. Figueroa, J.D. Mason, E.S. Fry, Appl. Opt. **54**, 334 (2015)
14. Avian Technologies LLC, http://www.aviantechnologies.com/products/coatings/highreflectance.php
15. E.S. Fry, J. Musser, G.W. Kattawar, P.W. Zhai, Appl. Opt. **45**, 9053 (2006)
16. Q.M. Wang, Z.Z. Wang, T. Kamimoto, Y. Deguchi, S.L. Cao, D. Wen, D. Takahara, Spectrochim. Acta., Part A **265**, 120333 (2022)
17. Z.L. Wang, C.W. Tian, S.Y. Qian, Y.F. Yu, J. Chang, Q.D. Zhang, Y.W. Feng, H.F. Li, Z.B. Feng, Opt. Laser. Technol. **145**, 107483 (2022)
18. A. Pogány, O. Werhahn, V. Ebert, J. Quant. Spectrosc. Radiat. Transfer. **276**, 107884 (2021)

Cite this article as: Xue Zhou, Haiwei Li, Peng Hu, Effective optical path length measurement of integrating cavity using time-resolved spectroscopy and tunable diode laser absorption spectroscopy, Eur. Phys. J. Appl. Phys. **97**, 53 (2022)